

Modular Optical Nodes with Anylane Add-Drop for Spatial Division Multiplexed Networks

Che-Yu Liu,¹ David T. Neilson,² Roland Ryf,² S. J. Ben Yoo,³ and Jesse E. Simsarian²

¹ Department of Computer Science, University of California, Davis, CA 95616, USA

² Nokia Bell Labs, 600 Mountain Ave., New Providence, NJ 07974, USA

³ Department of Electrical and Computer Engineering, University of California, Davis, CA 95616, USA

cylu@ucdavis.edu

Abstract: We compare anylane add-drop optical nodes with modular architectures for spatial-division multiplexed (SDM) networks. By modifying open-source GNPpy for SDM, we present simulations that show lower blocking probability for networks that utilize anylane add-drop architectures. © 2023 The Author(s)

1. Introduction

As single-fiber wavelength division multiplexed (WDM) optical transport systems have essentially reached the Shannon capacity limit for C and L amplifier bands, continued capacity growth can be achieved in the spatial domain [1]. In this work, we focus on spatial optical switching nodes designed for metro and core terrestrial networks with highly-meshed topologies and dynamic, automated operational capabilities. We expect variability in the number of fibers deployed on different links in these networks, which makes spatial superchannels (i.e., spread across multiple spatial modes/cores/fibers) impractical or inefficient due to the potential mismatch between the number of spatial modes in a superchannel and the number of available spatial modes on different fiber links in the network. Alternatively, spectral superchannels with multiple wavelengths filling the entire band provide high-capacity interconnection with no spatial constraints and with the additional benefit of compatibility with existing optical transponders. The solution works on cables consisting of bundles of single-mode fiber, a transmission medium that is presently deployed by network operators. Fibers with multiple uncoupled cores can also be supported, and we call the ability of the optical nodes to adapt to different fiber types “flexfiber” optical networking.

Previous work described switching solutions for combined WDM-SDM optical networks [2]. Alternatively, the concept of hierarchical optical networks was discussed in [3] where the WDM layer has an SDM underlay that allows expressing spectral superchannels without wavelength-layer processing. The core-selective switch (CSS), described in [4], enables a similar node architecture for SDM as the wavelength selective switch-based reconfigurable add-drop multiplexer (ROADM) WDM nodes, but the CSS has the disadvantage that it is designed for multi-core fibers and lacks core interchange for through traffic. On the other hand, SDM node architectures based on matrix switches are compatible with bundled SMFs and can also be equipped with fan-in fan-out (FIFO) components for adaptation to multi-core fibers with uncoupled cores for flexfiber capability. In particular, scalable and modular distributed Clos node architectures can be constructed out of smaller sub-matrix switches (subMSes) [3].

In this work, we introduce a modular subMS-based add-drop section for distributed Clos type SDM switching nodes, which enables adding and dropping spectral superchannels to the SDM layer with anylane capability. Similar to the colorless, directionless, and contentionless (CDC) flexibility properties of wavelength add drops in ROADMs, anylane means that a spectral superchannel can reach any network facing fiber or core from any port of the anylane add-drop section. We present novel SDM node architectures with anylane add-drop sections and show the scaling of the node in terms of the number of switches. Furthermore, we modified the open-source optical route planning library, GNPpy [5], for SDM networks and present network simulations that show a large reduction in network blocking when the anylane add-drop section is utilized.

2. Modular Optical Nodes with Anylane Add-Drop Capability

Fig. 1 shows three different node architectures with subMSes utilized for the anylane add-drop switches (AAD-Ses). The modularity of the switches allows for single or multiple subMSes to be used for each direction in a growable architecture, where switches can be added as the number of directions increases. Using separate switches for each direction is also advantageous for routing working and protection paths to not share a common switch failure group. Fig. 1a shows multiple WDM transport systems “stacked” to have multiple fibers per direction. While the multiple WDM systems are optically disconnected for through traffic, the anylane add-drop switches connected to the multi-cast switches (MCSes) allow wavelengths to be added and dropped to any fiber from any AADS port. However, in a stacked WDM architecture, the number of wavelength selective switches (WSSes) scales rapidly as the number of parallel fibers, m increases since each bidirectional fiber pair requires two WSSes.

To improve the scaling of the number of required switches as m increases, Fig. 1b shows a space-switching distributed Clos architecture, where the modular midstage switches (MSes) are at different network nodes. Fewer

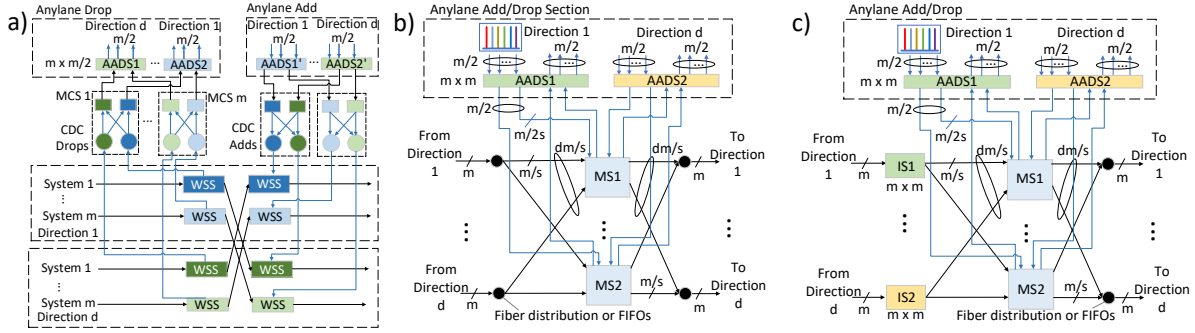


Fig. 1. Anylane add drop sections for a) Stacked WDM node b) Single-stage distributed Clos SDM node c) Two-stage distributed Clos SDM node

switches are required in total since each subMS acts on multiple fibers. The add and drop ports of the anylane add-drop section carry spectral superchannels, as indicated at the top of Fig. 1b and 1c, with spectral width up to the amplifier bandwidth. The incoming fibers are shuffled in groups of m/s fibers to the midstage switches (MSes), where s is the number of MSes [4]. The architecture is not non-blocking when one considers each fiber as an individual port because the number of midstage switches is insufficient, however, the redundancy of the multiple fibers per direction reduces the overall blocking in the network. The filled circles in Fig. 1b and 1c represent fiber distribution points, where fibers are redirected to implement the shuffle between the input fibers and midstage switches. In the case of bundled single-mode fibers, the distribution points would be simple fiber connectors, but for multi-core fibers fan-in fan-out tapered fiber bundles could be used to adapt the uncoupled cores of different types of multi-core fibers to the subMSes. Fig. 1c has input switches (ISes) which direct fibers to the MSes to allow automated implementation of the fiber shuffle. Normally, the IS fiber shuffle would be static, i.e., not be rearranged as connections are made. The modular subMS node solutions are preferable over a single large switch architecture because the modular designs have a lower startup cost [4], greater flexibility and scalability, and the smaller subMS footprints are compatible with existing optical transport shelves. Fig. 2a shows the average number of switches per node for an NSF15 network topology, where the types of switches are the sum of 1×20 WSSes and 64×64 matrix switches for the stacked WDM case of Fig. 1a, and only 64×64 matrix switches for the one- and two-stage architectures of Fig. 1b and 1c (i.e. IS, MS, and AADS are all 64×64 subMSes). The add-drop fraction at every node is 50% and the nodes are in-service growable to 8 directions. When the number of fibers per direction, $m = 20$, the average number of switches per node decreases from 126 (max in a 4-direction node = 164) for stacked WDM to 10 (max in a 4-direction node = 12) subMSes for two-stage distributed Clos. The savings in the number of switches become greater for larger m . The large reduction in the number of switches comes from the transition from wavelength to fiber switching.

3. SDM Network Simulations

To simulate the blocking performance of SDM networks, we made modifications to the open-source optical route planning library, GNPpy [5]. We added the capability of specifying the number of parallel fibers on each link in the network design stage, and multiple links in both directions are then automatically populated with unique names to the underlying graph model, NetworkX [6]. Three different network topologies were studied: 3-node ring (Fig. 2b), 4-node ring, and 6-node ladder (Fig. 2c). Each node consists of two midstage switches, MS1 and MS2, and an optional AADS that is added to the node in the simulations to give anylane add-drop capability and reduce network blocking. Each of the black lines interconnecting nodes in Fig. 2b and 2c represents 2 bidirectional fibers,

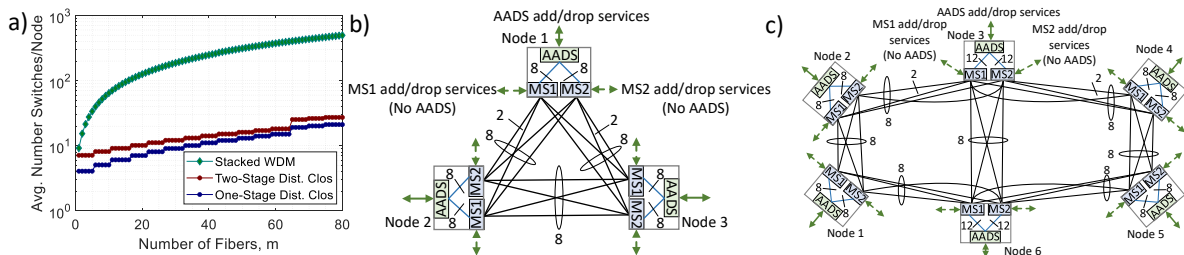


Fig. 2. a) Average number of switches per node for an NSF15 network topology b) 3-node ring and c) 6-node ladder topologies for network blocking simulations

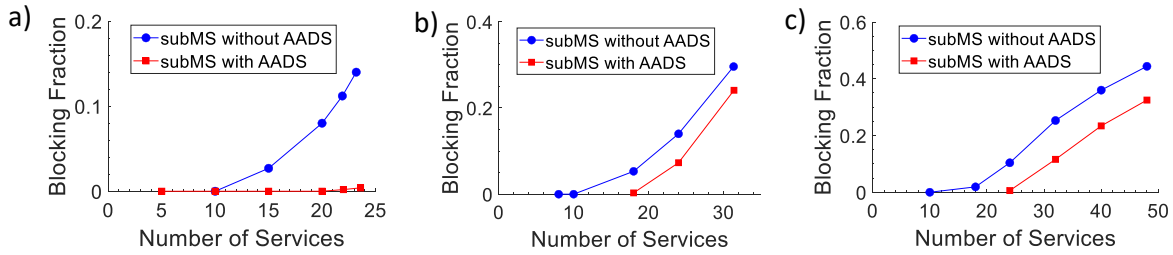


Fig. 3. The simulated blocking fraction versus number of full-spectrum superchannel services for a) 3-node ring network b) 4-node ring network c) 6-node ladder network

for a total of 8 bidirectional fibers per interconnection between nodes. The fibers are shuffled between the MSes at different nodes. Each fiber with a routed service is filled with a full-band spectral superchannel.

We compare the network blocking for the subMS nodes with and without the AADS by routing full-band spectral superchannel services that are randomly generated between nodes with a uniform distribution without exceeding the total available capacity between the AADS and MSes. The simulations sequentially route the services sent into/out of the AADS for the case with the AADS and into/out of the MSes for the case without the AADS (see Figs. 2b-c). The multiple parallel fibers per link cause an explosion in the number of paths in the network since we do not assume fiber (core) continuity as in [7]. For example, the 6-node ladder network with one fiber per internode link has 256 possible paths, which grows to 48.5 million paths for the 8-parallel fiber case of Fig. 2c. For the 3- and 4-node networks we executed the routing algorithm with NetworkX, a Python package used by GNPY. However, we achieved a large speedup ($\sim 500\times$ in one example case) by implementing the routing algorithm with the Cython/C++ NetworkKit [8] package, which reduced computation time for a large number of paths. Therefore, we compute all paths in the 6-node network with NetworkKit and perform path assignment with our own algorithm. Because each node is composed of multiple switches, “loop” paths that visit the same node more than once are generated when all paths are calculated. One of the main selection criteria for path assignment is to reject loop paths, including paths that traverse an AADS at intermediate nodes. The spectral superchannel services are routed on the shortest available first-fit fiber path. Each network blocking fraction calculation in the graphs of Fig. 3 is the average of 20 different runs of randomly generated services executed in parallel.

Fig. 3a shows the blocking fraction versus the number of services for the 3-node ring case of Fig. 2b. The blue curve of Fig. 3a is for the case without the AADS, where services are injected directly into MS1 and MS2 as indicated by the green dashed arrows in Fig. 2b. The blocking is higher because services may be injected into “mismatched” MSes on different nodes where no path is available between them. Using the AADS for the add/drop section of services drastically reduces this condition so that available paths are more likely to be found (red curve of Fig. 3a). Similar behavior can be observed for the 4-node ring, with the blocking results plotted in Fig. 3b, and 6-node ladder case (architecture shown in Fig. 2c and blocking simulation results shown in Fig. 3c). The overall reduction in blocking with the AADS becomes relatively smaller for the larger 4 and 6-node networks as more paths become available for the services added and dropped by the MSes to find routes between them.

4. Conclusions

We introduced architectures for stacked WDM and one- and two-stage distributed Clos SDM nodes with anylane add-drop sections, allowing spectral superchannels to be added and dropped to any fiber. The benefit of this capability was demonstrated by modifying GNPY to support SDM networks and performing simulations that show a large reduction in network blocking with the anylane add-drop capability.

References

1. P. J. Winzer and D. T. Neilson, “From Scaling Disparities to Integrated Parallelism: A Decathlon for a Decade,” *J. Lightwave Technol.*, 35, 5, 1099–1115, 2017.
2. D. M. Marom *et al.*, “Survey of Photonic Switching Architectures and Technologies in Support of Spatially and Spectrally Flexible Optical Networking,” *J. Opt. Commun. Netw.*, 9, 1, 1–24, 2017.
3. M. Jinno, “Spatial Channel Network (SCN): Opportunities and Challenges of Introducing Spatial Bypass Toward the Massive SDM Era,” *J. Opt. Commun. Netw.*, 11, 3, 1–14, 2019.
4. M. Jinno, “Spatial Channel Cross-Connect Architectures for Spatial Channel Networks,” *IEEE J. Sel. Top. Quantum Electron.*, 26, 4, 2020.
5. (2022), [Online], Available: <https://gnpy.readthedocs.io/en/master/>.
6. (2022), [Online], Available: <https://networkx.org/>.
7. A. Ferrari, E. Virgillito, V. Curri, “Networking merit of spatial-division and band-division multiplexing: A statistical assessment,” in *Proc. ICTON’20*, We.A1.1, 2020.
8. (2022), [Online], Available: <https://networkkit.github.io/>.